Int. J. Electrochem. Sci., 17 **(2022)** Article Number: 220453, doi: 10.20964/2022.04.32

International Journal of
ELECTROCHEMICAL
SCIENCE
www.electrochemsci.org

Short Communication

Effect of Particle Size of Li_3PO_4 on $LiFePO_4$ Cathode Material Properties Prepared by Hydrothermal Method

Yuan Ma[*], *Tao Li, Fei Jiang, Yuqi Jiang, Feilong Gao, Lingyun Liu, Yaodong Wu, Ying Meng, Xiaohang Ma, Zhenfa Zi*[*]

Key Laboratory for Photoelectric Detection Science and Technology of Education Department of Anhui Province, School of Physics and Materials Engineering, Hefei Normal University, Hefei 230601, People's Republic of China
[*]E-mail: mayuan@hfnu.edu.cn; zfzi@issp.ac.cn

Received: 18 December 2021 / *Accepted:* 3 February 2022 / *Published:* 4 March 2022

$LiFePO_4$ is one of the most widely used cathode materials for lithium ion batteries. $LiFePO_4$ prepared by hydrothermal method has the advantages of good consistency, small particle size, controllable morphology and accurate chemical ratio. In this paper, $LiFePO_4$ was prepared by hydrothermal method, and the effect of particle size of Li_3PO_4 as reaction raw material was studied. It is found that the particle size of Li_3PO_4 could affect the morphology and properties of $LiFePO_4$. Among the samples, the porous spherical structure of $LiFePO_4$ particles can be obtained by using 2 μm Li_3PO_4, which is assembled from nanoparticles. This $LiFePO_4$ has the best comprehensive performance and high vibration density.

Keywords: $LiFePO_4$; Li_3PO_4; Hydrothermal method; Particle size

1. INTRODUCTION

$LiFePO_4$ has been widely used as a cathode material for lithium-ion batteries since it was discovered by Goodenough's research group [1]. It has the advantages of high specific capacity (170 mAh/g), excellent stability, non-toxicity and low cost [2]. With the development of new energy vehicles and energy storage market, the $LiFePO_4$ will usher in further growth in the future. At present, the preparation methods of $LiFePO_4$ mainly include solid phase method [3-5], hydrothermal method [6-8], sol-gel method [9-11], coprecipitation method [12-14], etc. Among them, hydrothermal method is a common method to prepare nanometer particles [15]. It has the advantages of low reaction temperature, uniform mixing of raw materials, controllable particle size from nanometer to micron, and uniform and easy to control morphology [16]. It is expected to become one of the main methods for industrial production of high-performance $LiFePO_4$.

$FeSO_4$, LiOH and H_3PO_4 are commonly used as raw materials for the preparation of $LiFePO_4$ by hydrothermal method [17, 18]. The mixing of precursors involves multi-step reaction, and its complex reaction process increases the difficulty of reaction control and affects the consistency between batches of products. At the same time, because of its closed environment and high temperature and pressure, it is difficult to observe the material reaction process intuitively, and the reaction mechanism is still fuzzy. Therefore, to simplify the reaction process, in this paper, Li_3PO_4 as raw material is used to prepare $LiFePO_4$ by hydrothermal method, and the influence of Li_3PO_4 with different particle sizes on the product $LiFePO_4$ is studied.

2. EXPERIMENTAL SECTION

2.1 Materials and Methods

The raw material of Li_3PO_4 was self-made. The standard solutions of LiOH with concentrations of 0.6, 1.2 and 2.4 M were added to the corresponding quality of H_3PO_4 respectively, keeping the molar ratio of P to Li at 1:3. After stirring vigorously for 20 minutes, the white suspension was obtained, namely Li_3PO_4 suspensions with concentrations of 0.2, 0.4 and 0.8 M, respectively. The Li_3PO_4 solid particles in 0.2, 0.4 and 0.8 M suspensions were abbreviated as 1-LP, 2-LP and 3-LP.

$LiFePO_4$ was prepared by hydrothermal method. $FeSO_4·7H_2O$ and ascorbic acid (VC) were added to the lithium phosphate solution of 1-LP, 2-LP and 3-LP, respectively. The molar ratio of $FeSO_4$ to Li_3PO_4 was 1:1, and the reaction concentration of $FeSO_4$ after mixing was 0.2 M. VC was 10 wt.% of the theoretical yield of $LiFePO_4$. After sufficient stirring, the mixed solution was transferred to the hydrothermal reactor and reacted at 200℃ for 10 hours. After the reaction, the product was filtered, washed and dried. The obtained samples were thoroughly ground and mixed with 10 wt.% sucrose, and annealed at 650℃ for 10h in H_2/Ar (5 vol.% H_2) protective atmosphere to obtain $LiFePO_4$/C, which was named 1-LFP, 2-LFP and 3-LFP respectively.

2.2 Characterization

The crystal structure of the samples was analyzed by X-ray diffractometer (XRD, Bruker D8 Advance X-ray diffractometer). The surface morphology of the samples was observed by field emission-scanning electron microscope (SEM, Hitachi FE-SEM-4800). The tap density of the samples were tested by tap density tester (LABULK 0335).

2.3 Electrochemical measurements

The battery performances of the samples were tested through assembling the sample into 2032-coin cell. First of all, the cathode slurry was configured according to the weight ratio of samples, PVDF and acetylene black at 8:1:1, and mixed evenly with NMP as the solvent. The mixed slurry was spread evenly on an aluminum foil and dried at 80°C for 12 hours. After that, the aluminum foil with the slurry was compacted and cut into an electrode with a 12 mm diameter. The prepared electrode was assembled

into 2032-coin cell in the glove box, with lithium metal plate as the negative electrode, 1 mol/L $LiPF_6$ dissolved in ethylene carbonate (EC)/dimethyl carbonate (DMC) (1:1 v/v) as the electrolyte and Celgard 2250 as the separator. After the assembly, the cell was stand for 12 hours to be tested. All the constant current charge and discharge test were measured between 2.0 and 4.2 V (versus Li^+/Li) by battery measuring systems (NEWARE CT3008 multichannel battery measuring device) at room temperature.

3. RESULTS AND DISCUSSION

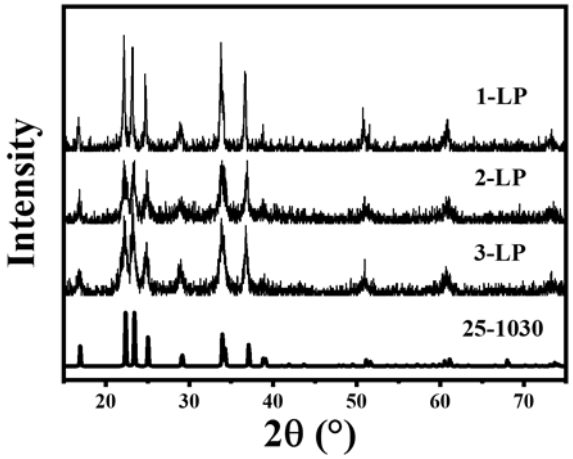

Figure 1. XRD pattern of the as-prepared Li_3PO_4 samples.

The XRD pattern of the as-prepared Li_3PO_4 was analyzed. As shown in Figure 1, the peak position and relative strength of the diffraction peak of the sample are basically consistent with the standard spectrum of Li_3PO_4 (PDF No. 25-1030), and there are no obvious impurity peaks, indicating that pure Li_3PO_4 has been prepared. By comparing the XRD pattern of three samples, it is found that the peak strength and half peak width are different. 3-LP prepared at high concentration has lower diffraction peak intensity and wider half peak width than 1-LP prepared at low concentration. According to Scherer's formula, the wider the full width at half maximum is, the smaller the particle size of the sample is [19]. The intensity of XRD diffraction peak is lower, the crystallization of the sample is worse [20]. Therefore, it can be inferred that the particle size of Li_3PO_4 prepared at high concentration is small, while that prepared at low concentration is large.

The morphology of the samples was observed by SEM, as shown in Figure 2. All the Li_3PO_4 samples are uniform spherical secondary particles composed of nanoparticles. The particle size of spherical secondary particles increases with the decrease of reaction concentration. The secondary particle size of 1-LP, 2-LP and 3-LP are about 2 μm, 1 μm and 200-300 nm, respectively. The primary particle size also has similar phenomenon. The primary particle size of 1-LP, 2-LP and 3-LP are about 80 nm, 50 nm and 20 nm, respectively. The result is consistent with the result of XRD.

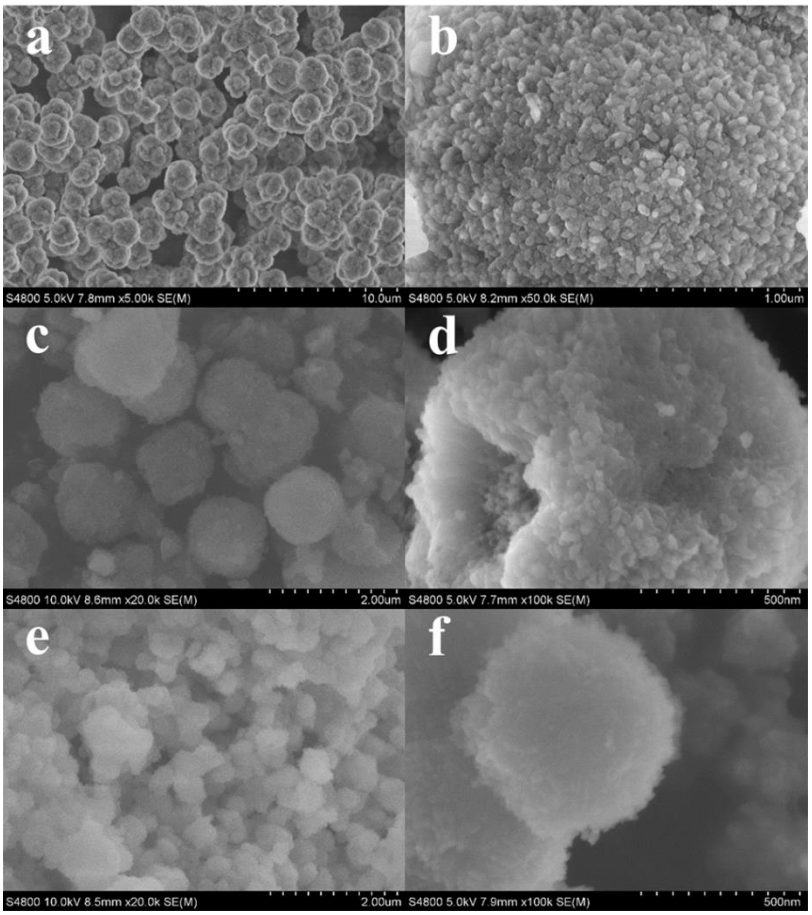

Figure 2. SEM images of (a, b) 1-LP, (c, d) 2- LP and (e, f) 3-LP.

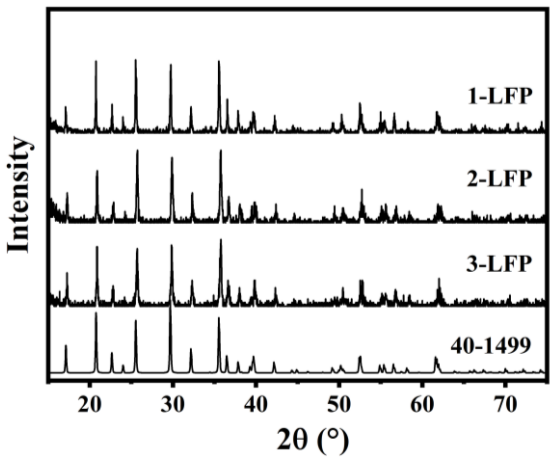

Figure 3. XRD patterns of the as-prepared $LiFePO_4$ samples.

Figure 3 shows the XRD patterns of $LiFePO_4$ prepared by 1-LP, 2-LP and 3-LP, and the standard XRD patterns of $LiFePO_4$ (PDF No. 40-1499). All diffraction peaks of the as-prepared samples are indexed to $LiFePO_4$, and no impurity phases could be observed, indicating that $LiFePO_4$ has been successfully prepared. By comparing the XRD patterns of 1-LFP, 2-LFP and 3-LFP, it can be seen that

the diffraction intensity is different, which indicates that the grain orientation of the samples is different, which can be further proved by SEM.

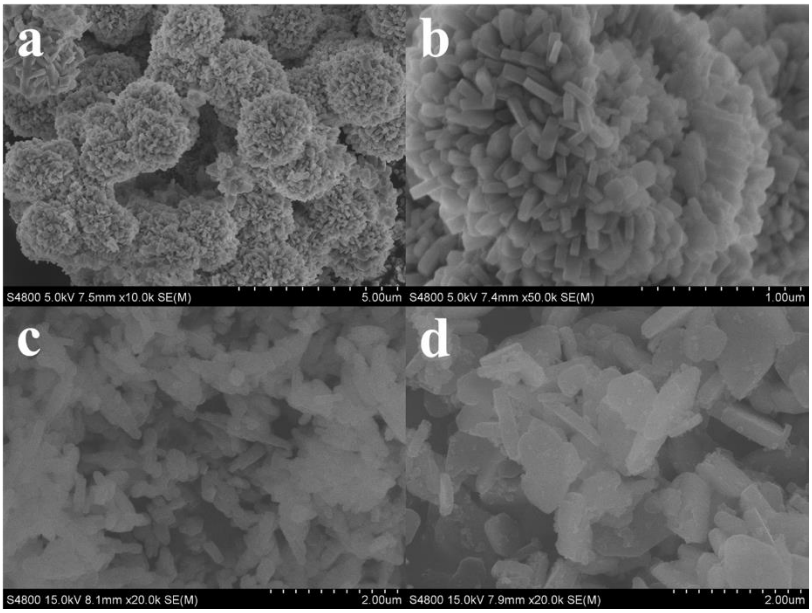

Figure 4. SEM images of (a, b) 1-LFP, (c) 2-LFP and (d) 3-LFP.

Figure 4 is the SEM diagram of the as-prepared $LiFePO_4$. The morphology of $LiFePO_4$ samples prepared by Li_3PO_4 with different particle sizes are different. 1-LFP is a porous spherical structure about 2 microns in diameter, composed of 100-200 nm particles. 2-LFP is a short rod of 0.5~1 μm. 3-LFP has a plate structure with a thickness of 200-300 nm.

After mixing Li_3PO_4 and $FeSO_4$, Li_2SO_4 and $FePO_4$ will be form, and two thirds of the Li_3PO_4 reactant will be consumed. The chemical reaction equation is as follows:

$$Li_3PO_4 + FeSO_4 \rightarrow Fe_3(PO_4)_2 \downarrow + Li_2SO_4 \quad (1)$$

The $LiFePO_4$ will be synthesized by hydrothermal treatment [21], according to the following reaction:

$$Fe_3(PO_4)_2 + Li^+ \rightarrow LiFePO_4 \downarrow \quad (2)$$

It can be speculated that 1-LFP basically maintains the spherical structure of 1-LP, due to the large size of 1-LP, which causes the reaction process of dissolution-reaction-precipitation react mainly at the surface of Li_3PO_4 [22, 23]. For the plate structure of 3-LFP, 3-LP has small size and disperses homogeneously during the reaction process, which could be approximated as a liquid phase. It can be known that $LiFePO_4$ prepared by hydrothermal method can easily form this structure [24, 25]. Between the above two cases, 2-LP is not enough to maintain its original morphology during the reaction, and 2-LFP forms a rod-like structure.

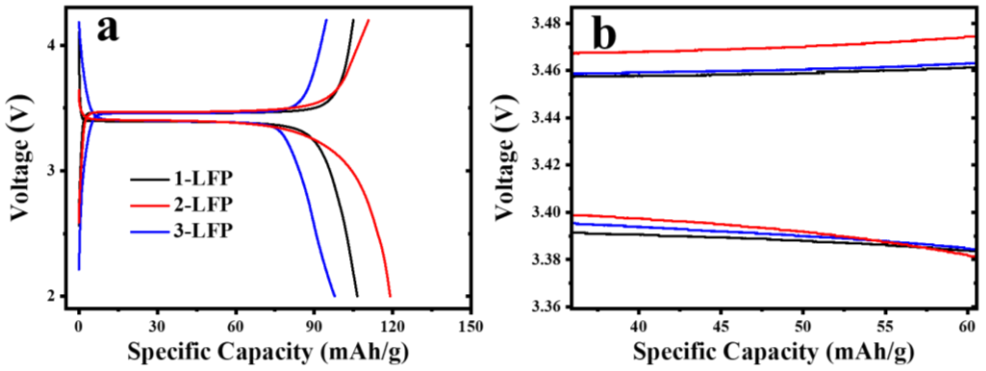

Figure 5. (a) Charge–discharge curves of the samples at a rate of 0.1 C and (b)the magnified image of the flat regions.

The charge and discharge test of the samples at 0.1C rate is shown in Figure 5a. The specific capacity of 2-LFP is the highest, which is 119.0 mAh/g. The specific capacity of 3-LFP was the lowest, 97.7 mAh/g. The specific capacity of 1-LFP is 112.4 mAh/g. Compare the potential difference of the charge and discharge platform as shown in Figure 5b, the potential difference of 2-LFP is the largest, indicating that its polarization is the largest. In general, nanocrystalization helps improve the lithium ion mobility of $LiFePO_4$, but too small particle size can be not good at carbon coating and the formation of conductive networks. Therefore, all aspects must be considered to obtain the best comprehensive performance.

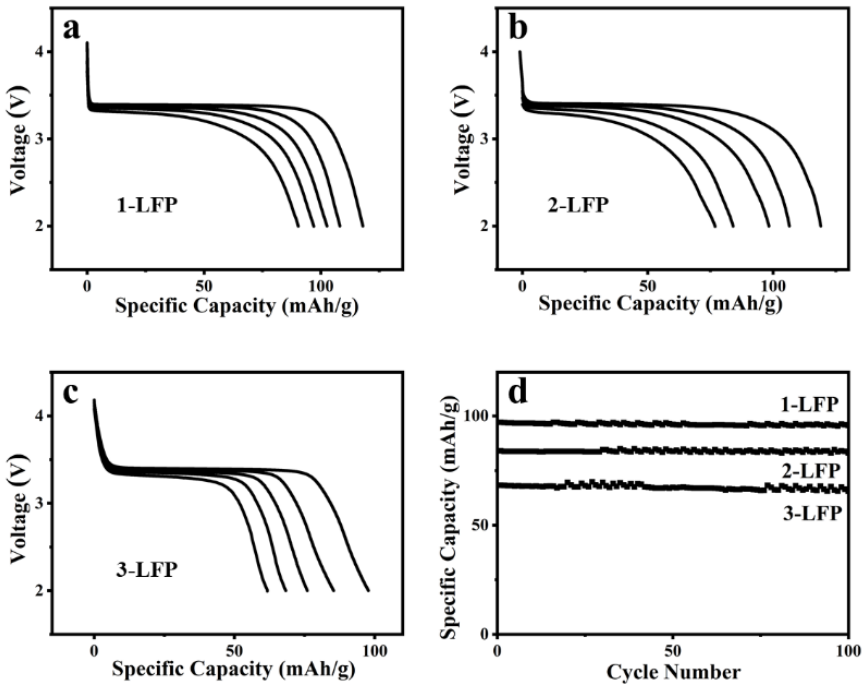

Figure 6. Discharge curves of (a) 1-LFP, (b) 2-LFP and (c) 3-LFP at various rates:0.1, 0.2, 0.5, 1.0 and 2.0 C; and (d) cycling performance of the samples at a rate of 1 C.

Figure 6 shows the discharge curves of the sample at 0.1, 0.2, 0.5, 1.0 and 2.0 C, and the cyclic test at 1 C. With the increase of the rate, the specific capacity of the samples decreases, which is caused by the polarization. By the comparison, 1-LFP has the best rate performance, which is 97.1 mAh/g at the 2 C and remains at 76.5% compared with the specific capacity at 0.1 C. The specific capacities of 2-LFP and 3-LFP at 2 C are 79.6 and 61.7 mAh/g, and the capacity retention are 66.9% and 63.1%, respectively. Figure 6d shows that the specific capacity of the sample does not decrease significantly after 100 cycles, which is determined by the stability of the crystal structure of $LiFePO_4$ [26]. Among them, the capacity retention rate of 1-LFP is 98.6%. 2-LFP and 3-LFP are 97.8% and 96.2%. 1-LFP has the best rate performance and cycle performance.

Table 1. The result of tap density of the samples

Sample	tap density (g/cm^3)
1-LFP	1.16
2-LFP	0.89
3-LFP	0.98

The tap density of $LiFePO_4$ must be considered in industrial production. Both carbon coating and nanocrystalization contribute to the improvement of the cell performance of materials, but at the same time cause the reduction of the tap density [27, 28]. The tap density of the sample is shown in Table 1. The tap densities of 1-LFP, 2-LFP and 3-LFP are 1.16, 0.89 and 0.98 g/cm^3, respectively. 1-LFP has the highest tap density, which helps to improve the energy density, due to the porous spherical structure and large grain size [29-31].

Table 2 shows $LiFePO_4$ is prepared using Li_3PO_4 as raw material by different methods. It can be seen that Li_3PO_4 could be used as raw material to prepare $LiFePO_4$, which obtain good specific capacity [32-35]. The hydrothermal method in literature is similar to this work, but the reaction conditions are different [32]. For example, Li_3PO_4, that has high degree of crystallinity and a fusiform shape with the length of 1 μm and width of 500 nm, was prepared through Na_3PO_4 reacted with LiCl that recovered from $LiFePO_4$. Meanwhile, the synthesized $LiFePO_4$ in literature was mixed with 12 wt.% of glucose to form carbon coating, which more than that in this work. The as-prepared $LiFePO_4$/C has relatively regular cuboid with the length of 200 nm and width of 100 nm, which is smaller. So, due to the faster lithium-ion mobility and better electrical conductivity, the $LiFePO_4$ has better electrochemical performance, compare to that in this work. However, the purpose of this work is to illustrate the effect of particle size of Li_3PO_4.

Table 2. Preparation methods of $LiFePO_4$ using Li_3PO_4 as raw material

Synthesis method	Sources of Li, P and Fe	Specific capacity	Reference
Hydrothermal method	Li_3PO_4 and $FeSO_4·7H_2O$	112.4 mAh/g at 0.1 C, 97.1 mAh/g at 2 C	This work
Hydrothermal method	Li_3PO_4 and $FeSO_4·7H_2O$	157.2 mAh/g at 0.2 C, 146.2 mAh/g at 1C, 122.4 mAh/g at 5 C	[32]
Solid state method	Li_3PO_4, $FePO_4$ and Fe powder	About 150 mAh/g at 0.1C, about 110 mAh/g at 5C	[33]
Spray-pyrolysis method	Li_3PO_4, $Fe(NO_3)_3$, and H_3PO_4	161.3 mAh/g at 1C	[34]
Solvothermal method	Li_3PO_4 and $FeSO_4·7H_2O$	168 mAh/g at 0.1C, 142 mAh/g at 1C	[35]

4. CONCLUSION

In summary, $LiFePO_4$ was successfully prepared by hydrothermal method with Li_3PO_4 as raw material, and the particle size of Li_3PO_4 had an effect on the performance of as-prepared $LiFePO_4$. By using different particle sizes of Li_3PO_4, rod-shaped, plate-shaped and porous spherical structures were obtained. Rod-shaped 2-LFP had small particle size and high specific capacity, but poor rate performance. The porous spherical structure of 1-LFP had good comprehensive performance, especially good rate performance and high tap density. Li_3PO_4 as raw material can provide lithium source and phosphorus source at the same time, reducing the type of reactants in hydrothermal process, and improving the utilization rate of raw material. And It is expected to be widely used in the production of lithium iron phosphate.

ACKNOWLEDGEMENTS
This work was supported by Universities Joint Key Laboratory of Photoelectric Detection Science and Technology in Anhui Province (No. 2020GDTC03), the Scientific Research Start-up Fund for Introduction of High-level Talents of HFNU (No. 2020rcjj05), the University Natural Science Research Project of Anhui Province (No. KJ2021A0911) and R&D Projects for Shandong Keyuan New Material Co., Ltd. (No. HXXM2021009).

References

1. A. K. Padhi, K. S. Nanjundaswamy and J. B. Goodenough, *J. Electrochem. Soc.*, 144 (1997) 1188.
2. M. S. Whittingham, *Chem. Rev.*, 104 (2004) 4271.
3. O. Cech, O. Klvac, P. Benesova, J. Maca, P. Cudek and P. Vanysek, *J. Energy Storage*, 22 (2019) 373.
4. H. Liu, S. H. Luo, S. X. Yan, Y. F. Wang, Q. Wang, M. Q. Li and Y. H. Zhang, *J. Electroanal. Chem.*, 850 (2019) 113434.
5. Z. M. Ma, R. G. Xiao, X. Liao and Y. Huang, *Ionics*, 25 (2019) 5669.

6. B. F. Zhang, Y. L. Xu, J. Wang, X. N. Ma and W. Q. Hou, *ACS Appl. Energ. Mater.*, 3 (2020) 5893.
7. F. Ruiz-Jorge, A. Benitez, S. Fernandez-Garcia, J. Sanchez-Oneto and J. R. Portela, *Ind. Eng. Chem. Res.*, 59 (2020) 9318.
8. W. L. Kong, Y. J. Gu, H. Q. Liu, Y. B. Chen, J. Yang and C. Q. Liu, *Int. J. Electrochem. Sc.*, 13 (2018) 2596.
9. M. A. M. M. Alsamet and E. Burgaz, *Electrochim. Acta*, 367 (2021) 137530.
10. C. H. Lu, W. Y. Li, T. Subburaj, C. Y. Ou and P. S. Kumar, *Ceram. Int.*, 45 (2019) 12218.
11. S. S. Jiang and Y. S. Wang, *Solid State Ionics*, 335 (2019) 97.
12. K. P. Wu, S. Yin, S. Wang, J. L. Zhu and W. T. Yao, *Carbon*, 169 (2020) 55.
13. X. Y. Wang, L. Z. Wen, Y. Zheng, X. Ren, Y. S. Li and G. C. Liang, *Ionics*, 26 (2020) 4433.
14. Y. L. Yan, Q. L. Li, B. Ren, R. Yang, Y. H. Xu, L. S. Zhong and H. Wu, *Ionics*, 24 (2018) 671.
15. J. A. Darr, J. Zhang, N. M. Makwana and X. Weng, *Chem. Rev.*, 117 (2017) 11125.
16. B. Q. Zhang, S. Z. Wang, Y. H. Li, P. P. Sun, C. Yang, D. Wang and L. Liu, *Ceram. Int.*, 46 (2020) 27922.
17. F. Ruiz-Jorge, A. Benitez, M. B. Garcia-Jarana, J. Sanchez-Oneto, J. R. Portela and E. J. Martinez de la Ossa, *Nanomaterials (Basel)*, 11 (2021) 2412.
18. H. T. Zhu, C. Miao, R. T. Guo, Y. Liu and X. Y. Wang, *Int. J. Electrochem. Sc.*, 16 (2021) 210331.
19. G. Yang, H. Ji, X. Miao, A. Hong and Y. Yan, *J. Nanosci. Nanotechnol.*, 11 (2011) 4781.
20. X. M. Lou and Y. X. Zhang, *J. Mater. Chem.*, 21 (2011) 4156.
21. X. Wang, X. Wang, R. Zhang, Y. Wang and H. Shu, *Waste Manag.*, 78 (2018) 208.
22. W. Xiang, E. H. Wang, M. Z. Chen, H. H. Shen, S. L. Chou, H. Chen, X. D. Guo, B. H. Zhong and X. L. Wang, *Electrochim. Acta*, 178 (2015) 353.
23. S. Yang, M. Hu, L. Xi, R. Ma, Y. Dong and C. Y. Chung, *ACS Appl. Mater. Inter.*, 5 (2013) 8961.
24. C. Y. Nan, J. Lu, L. H. Li, L. L. Li, Q. Peng and Y. D. Li, *Nano Res.*, 6 (2013) 467.
25. Y. J. Gu, C. J. Li, Long-Cheng, P. G. Lv, F. J. Fu, H. Q. Liu, J. X. Ding, Y. M. Wang, Y. B. Chen, H. F. Wang and S. W. Fan, *J. New. Mat. Electr. Sys.*, 19 (2016) 33.
26. L. X. Yuan, Z. H. Wang, W. X. Zhang, X. L. Hu, J. T. Chen, Y. H. Huang and J. B. Goodenough, *Energ. Environ. Sci.*, 4 (2011) 269.
27. Z. H. Chen and J. R. Dahn, *J. Electrochem. Soc.*, 149 (2002) A1184.
28. H. Gong, H. R. Xue, T. Wang and J. P. He, *J. Power Sources*, 318 (2016) 220.
29. C. Sun, S. Rajasekhara, J. B. Goodenough and F. Zhou, *J. Am. Chem. Soc.*, 133 (2011) 2132.
30. J. Su, X. L. Wu, C. P. Yang, J. S. Lee, J. Kim and Y. G. Guo, *J. Phys. Chem. C*, 116 (2012) 5019.
31. Y. Ma, X. L. Li, S. F. Sun, X. P. Hao and Y. Z. Wu, *Int. J. Electrochem. Sc.*, 8 (2013) 2842.
32. X. Wang, X. Wang, R. Zhang, Y. Wang and H. Shu, *Waste Manage.*, 78 (2018) 208.
33. C. Shen, G. Li, L. Liu, P. Li, H. Xu, H. Hu and L. Wang, *J. Power Sources*, 496 (2021) 229759.
34. J. Im, K. Heo, S.-W. Kang, H. Jeong, J. Kim and J. Lim, *J. Electrochem. Soc.*, 166 (2019) A3861.
35. J. Lu, W. Li, C. Shen, D. Tang, L. Dai, G. Diao and M. Chen, *Ionics*, 25 (2019) 4075.